

(Invited paper)

# Stability limits for spatial gap solitons in periodically modulated Bragg gratings

Boris A. Malomed

Department of Physical Electronics, School of Electrical Engineering, Faculty of Engineering,  
Tel-Aviv University, Tel-Aviv 69978, Israel

Manuscript received June 2, 2010

Revised June 10, 2010

## ABSTRACT

*We introduce a system of nonlinear coupled-mode equations (CMEs) for Bragg gratings (BGs) where the Bragg reflectivity periodically switches off and on as a function of the evolution variable. The model may be realized in a planar waveguide with the Kerr nonlinearity, where the grating is represented by an array of parallel dashed lines (grooves), aligned with the propagation direction. In the temporal domain, a similar system can be derived for matter waves trapped in a rocking optical lattice. Using systematic simulations, we construct families of gap solitons (GSs) in this system, starting with inputs provided by exact GS solutions in the averaged version of the CMEs. Four different regimes of the dynamical behavior are identified: fully stable, weakly unstable, moderately unstable, and completely unstable solitons. The analysis is reported for both quiescent and moving solitons (infact, they correspond to untilted and tilted beams in the spatial domain). Weakly and moderately unstable GSs spontaneously turn into persistent breathers (the moderate instability entails a small spontaneous change of the breather's velocity). Stability regions for the solitons and breathers are identified in the parameter space. Collisions between stably moving solitons and breathers always appear to be elastic. © 2010 Optical Society America*

OCIS codes: 050.2770, 230.1480, 190.5530, 060.5530

**Keyword** : *Optical, solitons*

## 1. INTRODUCTION AND THE MODEL

Bragg gratings (BGs) represent one of basic types of media used in photonics. They are written as periodic

lattices of defects on the surface of optical waveguides, such as fibers or thin films. With spatial period  $\lambda/(2\cos\alpha)$  where  $\alpha$  is the angle between the Poynting vector of the electromagnetic waves and the direction normal to grating (in particular,  $\alpha = 0$  in the case of the fiber grating, and  $0 < \alpha < \pi/2$  in planar waveguides, where the BG is realized as an array of parallel grooves), the BG provides for the resonant (Bragg) reflection of light, and thus linear interconversion between two waves co-propagating at wavelength  $\lambda$ . This mechanism gives rise to the bandgap in the corresponding spectrum, i.e., an interval of frequencies where linear waves cannot propagate. Fiber gratings have drawn a great deal of interest due to their important applications [1], such as optical sensors and elements used in fiber-optic telecommunications [2], and fundamental effects demonstrated by the wave dynamics in nonlinear gratings [3]– [7]. It was predicted that the combination of the strong effective dispersion near the bandgap and the Kerr nonlinearity of the waveguide may give rise to *gap solitons*, GSs (a more general name for them is “BG solitons”, as they are not necessarily centered inside the bandgap, in terms of the frequency domain) [5]. The standard model for the description of the light transmission through the nonlinear BG amounts to a system of coupled-mode equations (CMEs) for amplitudes of the two waves,  $u(x, t)$  and  $v(x, t)$ , which are linearly coupled by the Bragg reflection and interact nonlinearly via the cross-phase modulation, acting on themselves through the self-phase modulation [6]. The scaled form of the CME system is

$$iu_t + iu_x(|u|^2 + 2|v|^2)u + \kappa v = 0, \quad (1a)$$

$$iv_t + iv_x(|v|^2 + 2|u|^2)v + \kappa u = 0. \quad (1b)$$

In the case of the fiber grating,  $x$  and  $t$  are the coordinate along the fiber and time, while  $\kappa$  is the Bragg reflectivity. The group velocity of light and the overall Kerr coefficient are scaled to be 1. If  $\kappa$  is constant, it may also be replaced by 1.

A well-known two-parameter family of exact solutions for GSs is generated by Eqs. (1), with free parameters that determine the soliton's amplitude and velocity [4], [8], [9] [see Eqs. (4) below]. The stability of the GSs within the framework of Eqs.(1) was studied by means of the variational approximation [10], and then with the help of accurate numerical methods [11], [12]. The analysis had demonstrated that, approximately, half of the soliton family is stable, while the remaining part is unstable. Temporal solitons in short pieces of fiber gratings ( $\lesssim 10\text{cm}$ ) were created in the experiment, launching high-power laser pulses into the fiber [13]–[15].

GSs were also predicted as spatial solitons in planar waveguides [7], [24]–[26] and in photonic crystals [27]. Equations (2) are also relevant in that context, with  $t$  replaced by propagation coordinate  $z$ . Later, discrete GSs were predicted in discrete counterparts of CMEs (1) [16], [17]. Quasi-discrete spatial GSs were created in experiments, using arrays of semiconductor waveguides with strong cubic nonlinearity [18], [19], arrayed photovoltaic waveguides in LiNbO<sub>3</sub> [20], and photonic lattices with saturable nonlinearity [21]–[23].

Physical properties and potential applications of BGs may be vastly expanded by using gratings with various superstructures (alias supergratings), which, roughly speaking, amount to periodic variations of the Bragg reflectivity [coefficient  $\kappa$  in Eqs. (1)]. Superstructures have been investigated experimentally [28] and theoretically [29]. In particular, “coupled-supermode equations” were derived in Ref. [29], as a (rather complex) generalization of Eqs. (1). A specific Moiré superstructure, in the form of a sinusoidally modulated BG, was elaborated theoretically [30, 31] and realized in the experiment [32]. It features a narrow transmission band in the middle of the central gap, helping to create “slow light” in the grating. A superstructure pattern may also be implemented in the form the “semi-discrete” BG, i.e., as a waveguide with uniform nonlinearity and periodically placed short segments with strong Bragg reflectivity [33].

The form and stability of GS families in various models of fiber BGs with superimposed structures were studied in detail [29], [33]–[35]. In particular, it was found that the supergratings may open up additional bandgaps, populated by solitons, and they strongly affect the stability of the solitons. A similar result was demonstrated in the model of a Bose-Einstein

condensate (BEC) with the self-repulsive nonlinearity loaded into a periodic potential in the form of an optical lattice (OL). If a periodic long-wave modulation is imposed on the OL, it gives rise to additional “mini-gaps” in the linear spectrum, which may also be populated by specific types of GSs [36].

The objective of this work is to study the dynamics of spatial GSs in waveguides with the BG subjected to the “management” in the form of a periodic modulation of the reflectivity along the propagation distance,  $z$ . If the spatial grating is realized, as mentioned above, as a system of parallel grooves running along  $z$ , this simply means that the depth of the grooves varies periodically as a function of  $z$ . In particular, it is possible to consider the modulation of the piecewise-constant (Kronig-Penney) type, i.e., the spatial BG formed by an array of periodically “dashed” grooves. The respective scaled system of the CMEs is [cf. Eqs. (1)]

$$i \frac{\partial u}{\partial z} + i \frac{\partial u}{\partial x} + (|u|^2 + 2|v|^2)u + \kappa(z)v = 0, \quad (2a)$$

$$i \frac{\partial v}{\partial z} - i \frac{\partial v}{\partial x} + (|v|^2 + 2|u|^2)v + \kappa(z)u = 0, \quad (2b)$$

where, in the case of the Kronig-Penney (“on-off”) modulation, the management map is defined as follows, within its period  $Z_{map} \equiv Z_{on} + Z_{off}$ :

$$\kappa(Z_{map}) = \begin{cases} \kappa & 0 < z < Z_{on} \\ 0 & Z_{on} < z < Z_{on} + Z_{off} \end{cases} \quad (3)$$

We define the map so as to scale the the average reflectivity to 1, i.e.,  $\bar{\kappa} = \kappa Z_{on} / Z_{map} \equiv 1$ , hence  $\bar{\kappa} = \kappa Z_{map} / Z_{on} > 1$ . Setting  $\kappa = 1 (Z_{off} = 0)$ , makes Eqs. (2) identical to the standard system (2) with the uniform grating.

The difference of the present model from all previous studies of superstructures in BGs is that the reflectivity is periodically modulated as the function of the evolutionary variable ( $z$ ), while in earlier works the superstructures were represented by periodic functions of  $x$  [29], [33]–[36]. While the “Bragg management” of this type is obviously possible in the spatial domain, it is virtually impossible for temporal solitons, which were dealt with in the earlier works. Accordingly, the model based on Eqs. (2) and (3) belongs to the general class of *management systems*, in which one or several parameters are made periodic functions of the evolution

variable [38]. Previously, a different model of the management in the spatial-domain BG system was introduced in Ref. [37], where the local nonlinearity periodically jumped between self-focusing and self-defocusing along the propagation distance. Another physically relevant example of the management, which eventually leads to the same equations (2), but in the temporal domain, was experimentally realized in BEC, in the form of a “rocking” OL, i.e., the lattice which, as a whole, performs a periodic motion [39], [40] (in the spatial domain, a counterpart of the rocking lattice was experimentally realized in a planar waveguide carrying a periodically undulating BG [41]). If the intrinsic nonlinearity of the BEC is self-repulsive, which is the case in the experiment, this setting suggests to study stability limits for GSs trapped in the rocking OL, which was done in Ref. [42]. In particular, in the limit of a weak OL which performs the rocking motion with a large amplitude, the underlying one-dimensional Gross-Pitaevskii equation was reduced to Eqs. (2) with  $\kappa(t)$  represented by a periodic chain of delta-functions.

The paper is organized as follows. In Section 2, we report results of a systematic numerical analysis of “quiescent” GSs (i.e., untilted beams in the spatial domain). Four types of the dynamical behavior are identified: completely stable solitons; weakly unstable ones, which form robust breathers; moderately stable solitons, that lose a part of their power and turn into persistent moving breathers; and completely unstable beams, quickly decaying into radiation. Stability borders for the solitons and breathers are identified in relevant parametric planes. In Section 3, the analysis is extended to initially “moving” solitons (actually, tilted beams), which demonstrate similar types of the behavior. Their stability regions are identified too. In Section 3, we also briefly consider collisions between stable moving solitons. Section 4 concludes the paper.

## 2. STABILITY LIMITS FOR QUIESCENT SOLITONS

To look for soliton solutions in the present model, it is natural to start with initial conditions that would yield the usual exact GS solutions in the averaged version of Eqs. (2), i.e., Eqs.(1) with  $\kappa = 1$  [8], [9]:

$$u_0(x) = A^{-1}(\sin \delta)W \exp(i\sigma) \operatorname{sech}(\theta - i\delta/2), \quad (4a)$$

$$v_0(x) = -A(\sin \delta)W \exp(i\sigma) \operatorname{sech}(\theta + i\delta/2), \quad (4b)$$

where parameters  $\delta(0 < \delta < \pi)$  and  $c(-1 < c < +1)$

determine the amplitude and velocity of the GS (in fact, in the spatial domain “velocity” means a tilt of the beam carrying the soliton, relative to axis  $z$ ):

$$A = [(1-c)/(1+c)]^{1/4}, \gamma = (1-c^2)^{-1/2}, \quad (5)$$

$$\theta = \gamma(\sin \delta)(x - cz), \delta = \gamma(\cos \delta)(cx - z), \quad (6)$$

$$W = \sqrt{\frac{1-c^2}{3-c^2}} \left[ \frac{\exp(2\theta) + \exp(-i\delta)}{\exp(2\theta) + \exp(i\delta)} \right]^{\frac{2c}{3-c^2}}. \quad (7)$$

Integral characteristics of the soliton are its total power (which corresponds to the energy, in the temporal domain) and momentum (see, e.g., Ref. [43]),

$$E \equiv \int_{-\infty}^{+\infty} [|u(x)|^2 + |v(x)|^2] dx = 4\theta(1-c^2)/(3-c^2), \quad (8)$$

$$P \equiv i \int_{-\infty}^{+\infty} (u_x^* u + v_x^* v) dx = 4c\sqrt{1-c^2} \times \left[ \frac{7-c^2}{(3-c^2)}(\sin \delta - \delta \cos \delta) + \frac{\delta \cos \delta}{3-c^2} \right]. \quad (9)$$

The power and momentum, unlike the Hamiltonian, remain dynamical invariants of Eqs. (2) in the presence of the management,  $\kappa = \kappa(z)$ .

The known result is that, at  $c = 0$ , these GSs are stable, as solutions to Eqs. (1), in interval  $0 < \delta < \delta_{cr} \approx 0.505\pi$ , i.e., almost exactly in the half of their existence domain [10]–[12]. At  $c \neq 0$ , the dependence of  $\delta_{cr}$  on  $c$  is very weak [11].

Because the present model does not admit an analytical consideration, results for the existence and stability of GSs were collected from systematic simulations of Eqs. (2) with initial conditions (4). In this section, we summarize the findings for the quiescent GSs ( $c = 0$ ), i.e., in fact, for the spatial solitons which represent straight beams running parallel to axis  $z$ . The simulations reveal four distinct types of the dynamical behavior: full stability, weak instability, moderate instability, and complete instability, as specified below.

First, stable solitons with an almost permanent shape were found, being similar to their counterparts given by exact solution (4) with  $c = 0$ . A typical example of a completely stable soliton is displayed in Fig. 1. In most cases, the stable nearly-stationary soliton keeps at least 99.9% of the initial power, a tiny share being lost with emitted small-amplitude waves. Naturally, such solitons exist when the modulated model

is very close to the one with the constant reflectivity, i.e., for small values of  $\kappa - 1$ , see Eq. (3).

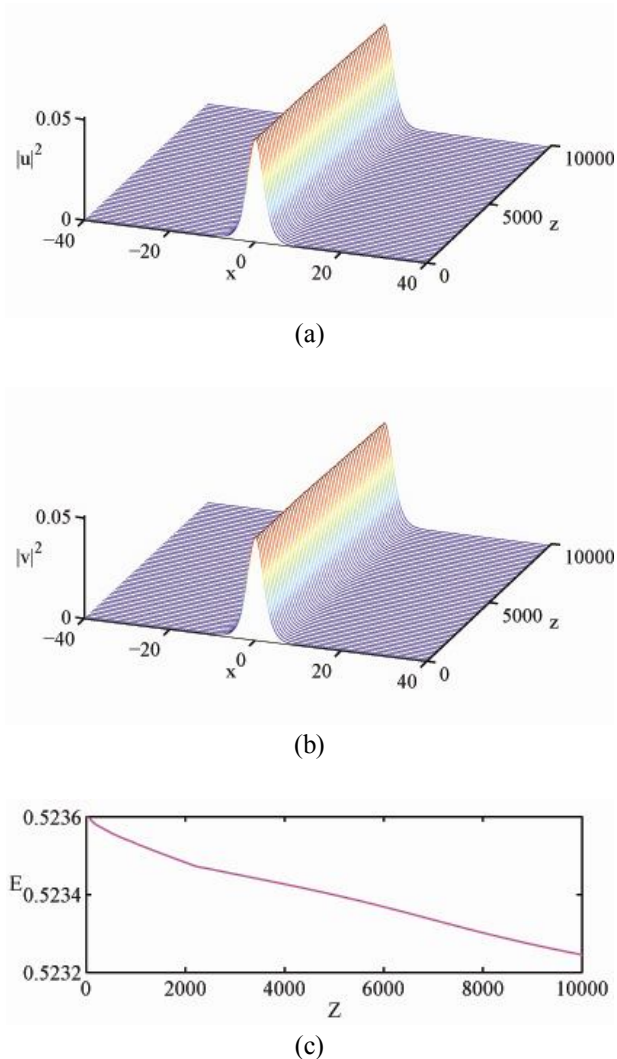


**Fig. 1.** (Color online) A typical example of a stable nearly-stationary quiescent soliton for  $\kappa = 1.01$ ,  $\delta = \pi/8$  and  $Z_{\text{map}} = 4.2$ . In this figure and Figs. 2-4 below, panels (a) and (b) display the evolution of the  $u$ - and  $v$ -components, respectively. Panel (c) shows the evolution of the soliton's power.

Weakly unstable solitons can be easily found too. They rearrange themselves into robust breathers, which then remain stable indefinitely long, see an example in Fig. 2. In most cases, the breathers keep no less than 98% of the initial power. Further, Fig. 3 demonstrates that a moderately strong instability originally converts the soliton into a breather-like mode, but, after a long evolution, it spontaneously breaks the reflectional symmetry, and starts moving slowly, and somewhat erratically, in either direction. The moving breathers,

although no longer being quiescent modes, keep their integrity until hitting an edge of the integration domain. The spontaneous onset of the motion of a moderately unstable soliton is not affected by the interaction with radiation waves, that were originally emitted by it and would eventually hit the soliton after bouncing back from edges of the computation domain, as the radiation was eliminated by absorbers installed at the edges. The size of the domain was made large enough, to avoid effects of absorbers on the solitons.

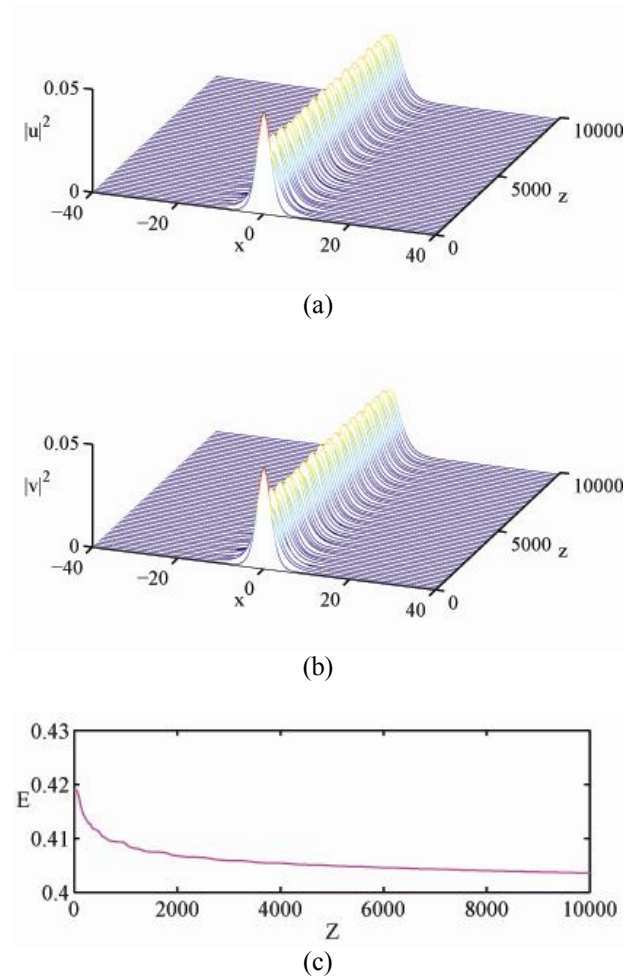


**Fig. 2.** (Color online) A typical example of a stable breather generated by the evolution of a weakly unstable quiescent soliton, for  $\kappa = 1.5$ ,  $\delta = \pi/10$  and  $Z_{\text{map}} = 1$ .

It may seem that the spontaneous onset of motion of the moderately unstable breathers violates the conservation of the momentum, see Eq. (9). However, Fig. 3 demonstrates that the actual value of the spontaneously acquired velocity is very small,  $c_{\text{spont}} \approx 0.008$ . Detailed inspection of the numerical data (not shown here) demonstrates that the small momentum

carried by the moving soliton is compensated by the recoil effect, i.e., by the momentum carried away by radiation waves emitted by the moderately unstable soliton in the course of its transformation.

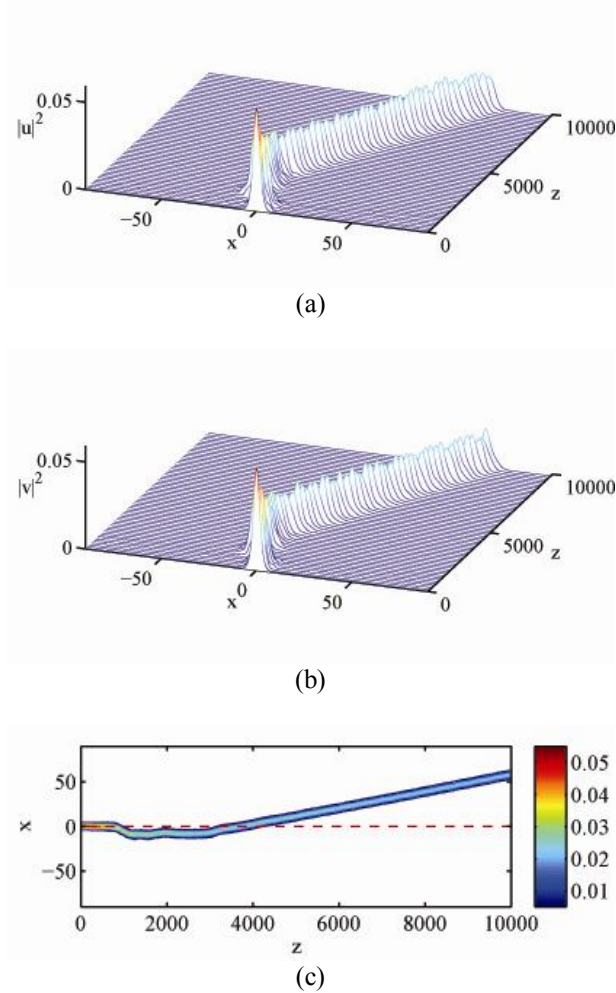


**Fig. 3.** (Color online) The evolution of a moderately unstable initially quiescent soliton, which spontaneously transforms itself into a moving breather, at  $\kappa = 1.15$ ,  $\delta = \pi/8$  and  $Z_{\text{map}} = 2.5$ . Panel (c) displays a detailed picture of the soliton's motion by means of contour plots of  $|u(x, z)|^2$  [for  $|v(x, z)|^2$  the picture is virtually identical].

Finally, Fig. 4 represents a typical example of the complete instability of solitons, which, naturally, occurs at sufficiently large values of the management period  $Z_{\text{map}}$  (when the BG is switched off for a long “time”), and/or large values of  $(\kappa - 1)$ . We stress that the solitons of all the types would survive or decay as a tightly bound states, without splitting into the  $u$ - and  $v$ -components.

Stability regions for the quiescent solitons and breathers, as well as the region of the existence of the moderately unstable solitons, are shown in Fig. 5 in the plane of  $(\delta, Z_{\text{map}})$  for fixed  $\kappa = 1.01, 1.1, 1.3$ , and  $1.7$  [see Eqs. (3) for the definitions], and in Fig. 6 in the plane of  $(\kappa - 1, Z_{\text{map}})$ , for fixed  $\delta = \pi/10$ . In Fig. 5(c) and 5(d), the “moderately unstable breathers” are essentially the same objects as the moderately unstable solitons defined above, i.e., spontaneously moving pulsating modes which maintain their integrity (after shedding off a part of the total power in the course of the initial evolution), and “decaying breathers” are the same as “decaying solitons”, being completely unstable objects. In Fig. 6, the vertical border between the stable solitons and breathers is a somewhat fuzzy one, as stable solitons too feature very small intrinsic oscillations.

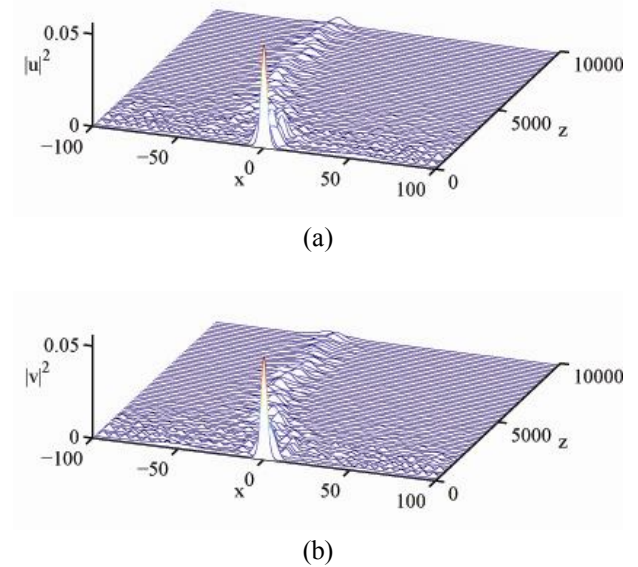


**Fig. 4.** (Color online) An example of the decay of a completely unstable quiescent soliton, for  $\delta = \pi/8$ ,  $\kappa = 1.1$ , and  $Z_{\text{map}} = 3.0$ .

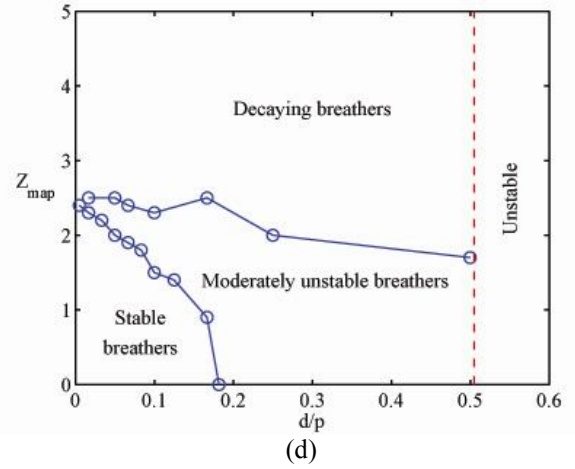
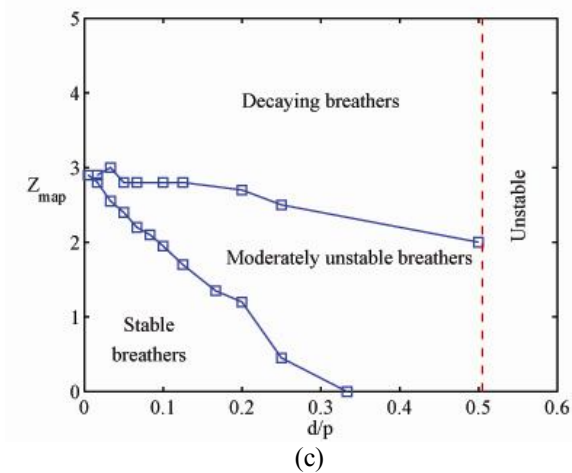
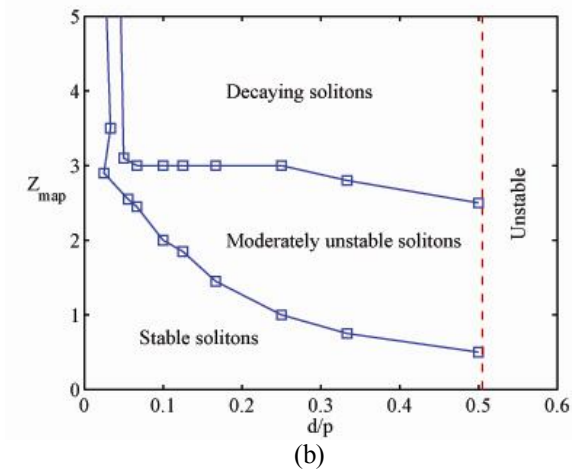
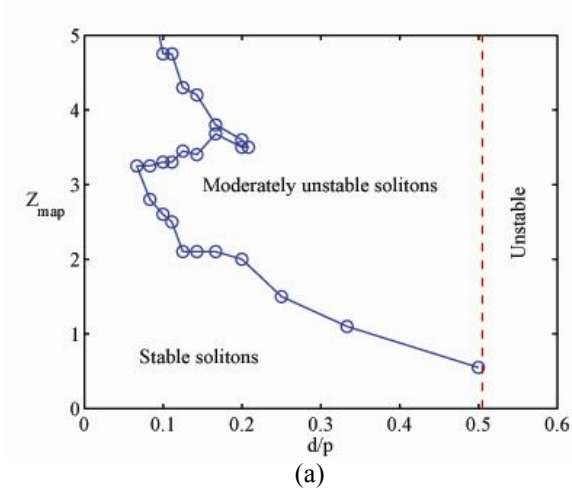


**Fig. 5.** (Color online) Stability borders for the (initially) quiescent solitons in the plane of  $(\delta, Z_{\text{map}})$  for fixed  $\kappa = 1.01$  (a), 1.1 (b), 1.3 (c) and 1.7 (d). In panel (a), which corresponds to very small  $\kappa - 1 = 0.01$ , the diagram does not have a region of completely unstable (decaying) solitons. The vertical lines at  $\delta \approx \pi/2$  represents the stability border in the standard model with the uniform reflectivity,  $\kappa(x) \equiv 1$  [10]–[12], see the text.

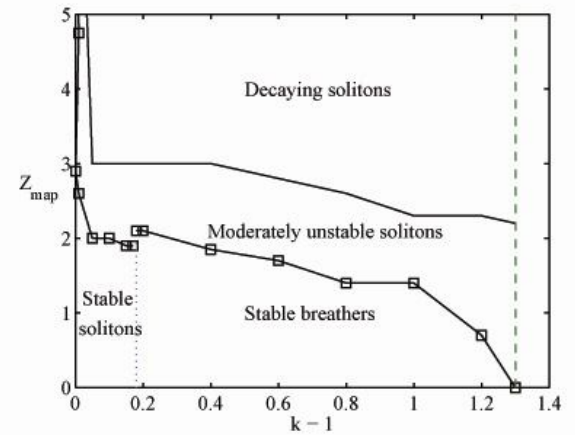


**Fig. 6.** (Color online) Stability borders for the (initially) quiescent solitons in the plane of  $(\kappa - 1, Z_{\text{map}})$  for fixed  $\delta = \pi/10$ .

### 3. MOVING GAP SOLITONS

#### 3.A. The stability of moving solitons

In experiments performed with temporal GSs in fiber gratings, only moving solitons have been created thus far [13]–[15]. As said above, in the spatial domain “moving” GSs, such as those given by Eq. (4), with  $c \neq 0$ ,

actually represent light beams tilted with respect the  $z$  axis. The creation of of both “quiescent” and “moving” (untilted and tilted) spatial quasi-discrete GSs was reported in arrays of parallel waveguides [19].

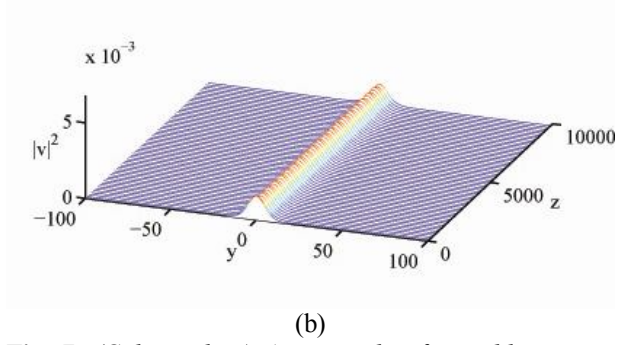
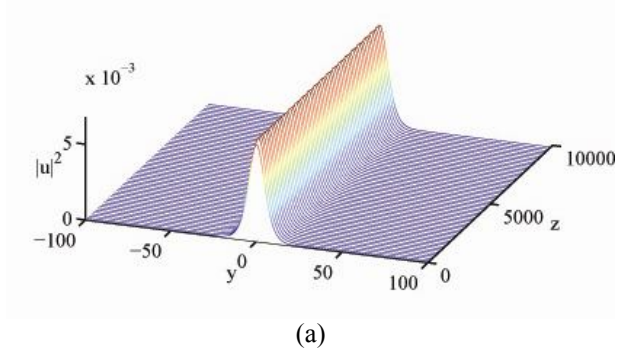


**Fig. 7.** (Color online) An example of a stable moving soliton generated by the initial condition (4) with  $\delta = \pi/30$ ,  $\kappa = 1.2$  and velocity parameter  $c = 0.6$  in initial conditions (4) (the actual average velocity produced by the simulations is  $\bar{c} \approx 0.667$ ). The management period is  $Z_{map} = 0.6$ . Here and in Figs. 8 and 9, coordinate  $y$  is defined as per Eq. (10), with appropriate values of  $\bar{c}$ .

We tried to generate moving solitons in the present model by running the simulations with the input in the form of expressions (4) with finite values of  $c$ . A technical problem is that, with the available size of the simulation domain, moving solitons may reach the domain’s edges and hit the absorbers. This problem could be easily solved in the following way: Running the simulations in the direct way until the soliton would hit the absorbers, the actual average velocity of the soliton,  $\bar{c}$ , was found from the numerical data [there is a difference between  $\bar{c}$  and parameter  $c$  in initial conditions (4), see below]. Then, Eqs. (2) were rewritten using the traveling coordinate,

$$y = x - \bar{c}z, \quad (10)$$

Instead of original  $x$ . The transformed equations take the following form :

$$i \frac{\partial u}{\partial z} + i(1 - \bar{c}) \frac{\partial u}{\partial y} + (|u|^2 + 2|v|^2)u + \kappa(z)v = 0, \quad (11a)$$

$$i \frac{\partial v}{\partial z} + i(1 + \bar{c}) \frac{\partial v}{\partial x} + (|v|^2 + 2|u|^2)v + \kappa(z)u = 0, \quad (11b)$$

and initial conditions (4) were transformed accordingly too. Then, solitons found as the numerical solutions to Eqs. (11) remained close to the initial position as long as the simulations were run, allowing us to make definite conclusions about their stability.

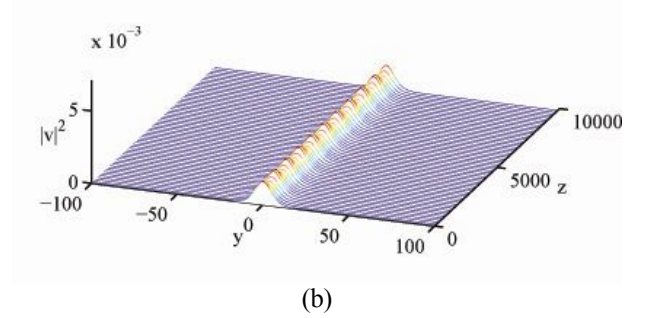
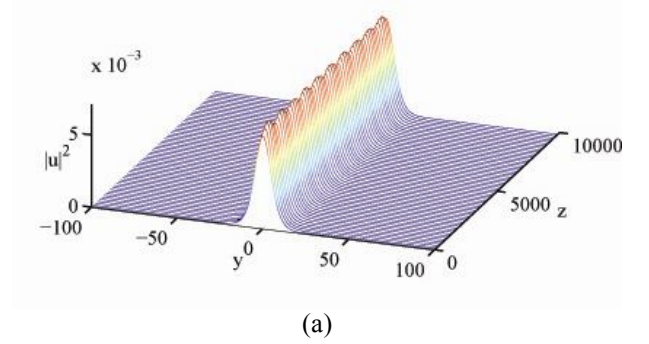


**Fig. 8.** (Color online) An example of a stable moving breather, with  $\delta = \pi/30$ ,  $\kappa = 1.2$ ,  $c = 0.6$  and  $Z_{map} = 1.2$ . The average velocity produced by the simulations is  $\bar{c} \approx 0.658$ .

The results again reveal four types of the dynamical behavior. Examples of stable moving solitons and breathers are shown in Figs. 7 and 8, respectively. As well as in the case of the quiescent solitons, the border between them is fuzzy, as any soliton in the present model performs some intrinsic oscillations. A counterpart of what was defined as moderately unstable breathers in the case of the initial condition with  $c = 0$

was found here too, see an example in Fig. 9. In the latter case, we observe the formation of breathers which lose a considerable part of their total power, and demonstrate deviations from the steady motion, with small acceleration and deceleration around the average velocity.

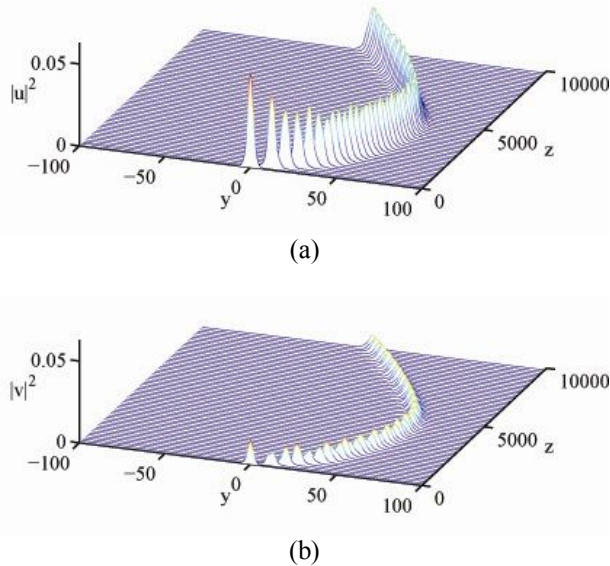


**Fig. 9.** (Color online) An example of moderately unstable moving breather, with  $\delta = \pi/10$ ,  $c = 0.6$ , and  $Z_{\text{map}} = 1.5$ ,  $\kappa = 1.2$ . The average velocity produced by the simulations is  $\bar{c} \approx 0.538$  (note that  $\bar{c} < c$  in this case, on the contrary to  $\bar{c} > c$  in the cases displayed in Figs. 7 and 9).

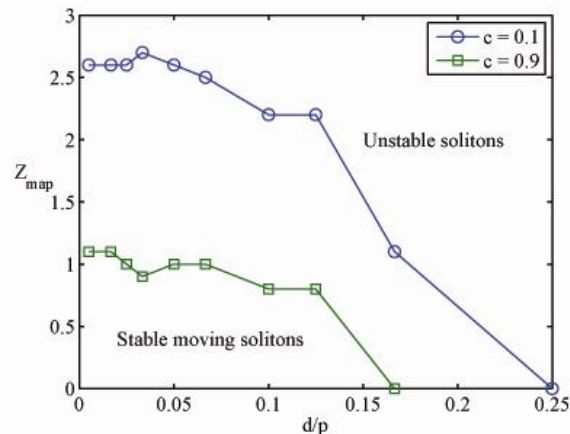


**Fig. 10.** (Color online) Stability borders for moving solitons with velocities  $c = 0.1$  and  $c = 0.9$ , at  $(\kappa - 1) = 0.01$ .

For very small values of  $(\kappa - 1)$  – for instance,  $\kappa - 1 = 0.01$  – the stability border for the moving

solitons with small and large velocities, *viz.*,  $c = 0.1$  and  $c = 0.9$ , are shown in Fig.10. In this case, stable breathers were not found, as a species visibly different from the stable solitons. On the contrary, at larger  $(\kappa - 1)$ , such as  $\kappa - 1 = 0.2$ , stable moving solitons with small velocities could not be generated, but stable moving breathers were found instead. This result complies with the above finding that, in the case of the zero velocity, stable breathers appear with the increase of  $(\kappa - 1)$ , see Fig. 6. The stability borders for this case are shown in Fig. 11(a), for  $c = 0.2$ .

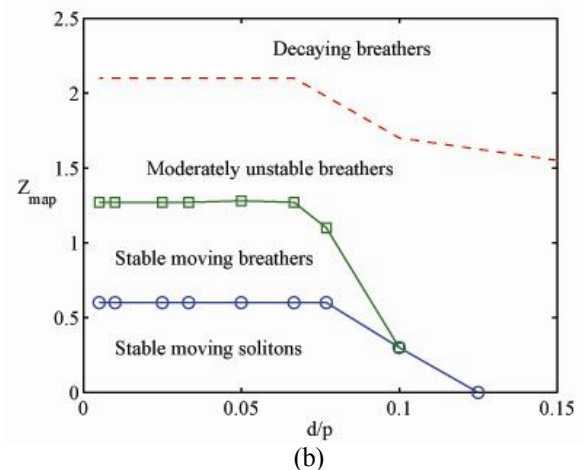
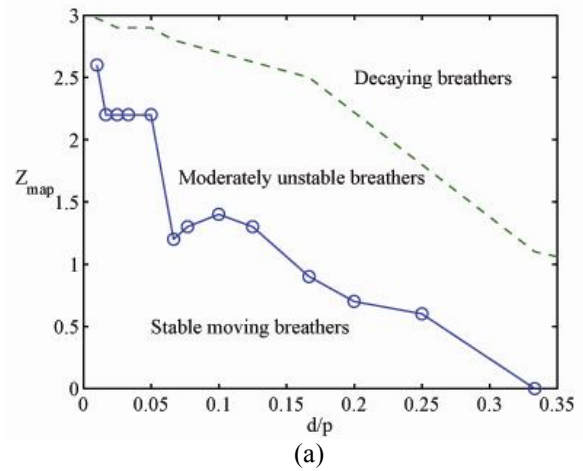


**Fig. 11.** (Color online) Stability borders for the moving solitons with  $\kappa - 1 = 0.2$ : (a)  $c = 0.2$ , (b)  $c = 0.6$ .

On the other hand, for intermediate velocities,  $c \approx 0.4 - 0.6$ , both stable moving solitons and breathers can be identified. The stability borders for  $c = 0.6$  (and  $\kappa - 1 = 0.2$ ) are displayed in Fig. 11(b). At velocities  $c > 0.6$ , no stable moving objects, solitons or breathers, could be found for  $\kappa - 1 = 0.2$ .

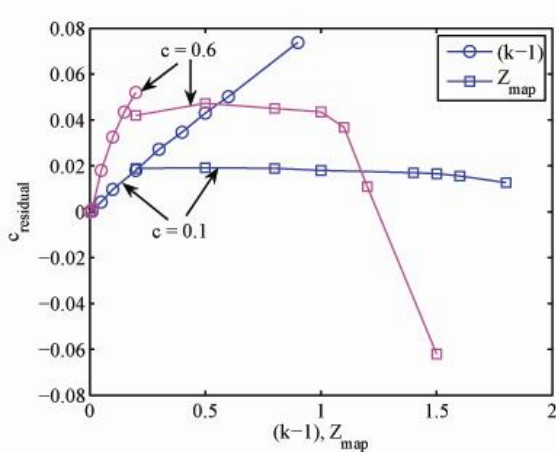


**Fig. 12.** (Color online) The residual velocity (defined in the text) as functions of  $\kappa - 1$  and  $Z_{\text{map}}$ , at fixed  $Z_{\text{map}} = 1$  and  $\kappa = 1.2$ , respectively. In both cases,  $\delta = \pi/10$ .

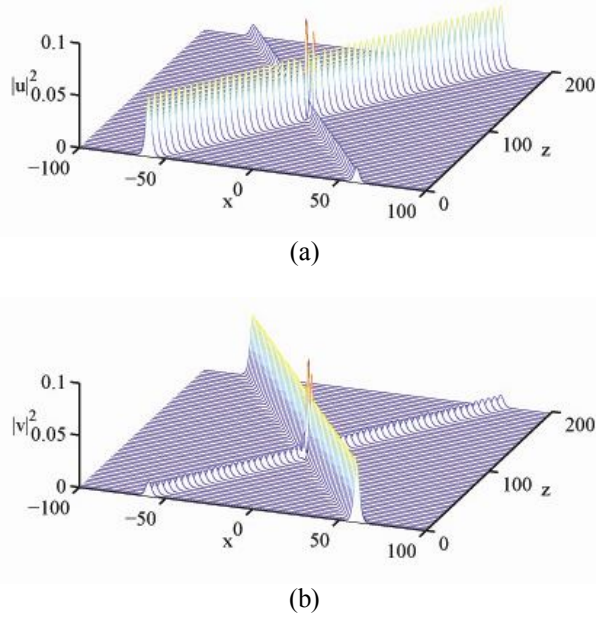


**Fig. 13.** (Color online) The collision between stable solitons moving with velocities  $c = \pm 0.6$ , the other parameters being  $\kappa - 1 = 0.2$ ,  $Z_{\text{map}} = 0.5$ , and  $\delta = \pi/10$ .

As said above, the average velocity  $\bar{c}$ , which could be extracted from the numerical data, was (slightly) different from the value of  $c$  in the initial conditions (4). For stable moving solitons, Fig. 12 shows the *residual velocity*,  $c_{\text{residual}} \equiv \bar{c} - c$ , versus  $(\kappa - 1)$  and  $Z_{\text{map}}$  for fixed  $\delta = \pi/10$ . Except for the point with the negative value,  $c_{\text{residual}} \approx -0.062$ , which corresponds to the moderately unstable breather displayed in Fig. 9 (for  $Z_{\text{map}} = 1.5$ ,  $\kappa = 1.2$  and  $\delta = \pi/10$ ,  $c = 0.6$ ), all other data

points, with  $c_{\text{residual}} > 0$ , pertain to stable solitons and weakly unstable breathers. One can see that the residual velocity of the stable and weakly unstable modes strongly depends on  $(\kappa - 1)$ , and weakly depends on the management period,  $Z_{\text{map}}$ .

### 3.B. Collisions between stable moving solitons

The availability of stable moving solitons suggests a possibility to consider collisions between them. In the standard model based on CMEs (1), collisions between moving GSs were studied in detail, by means of systematic simulations [44], [45]. The collisions were also studied in a generalized model that contains additional terms accounting for the dispersion of the Bragg reflectivity [46]. In the model of the superstructure represented by a chain of short BG segments, against the background of the uniform Kerr nonlinearity, collisions were studied in detail in Ref. [33]. In all these models, regions of quasi-elastic and strongly inelastic collisions, that might lead to merger of the colliding solitons, were identified.

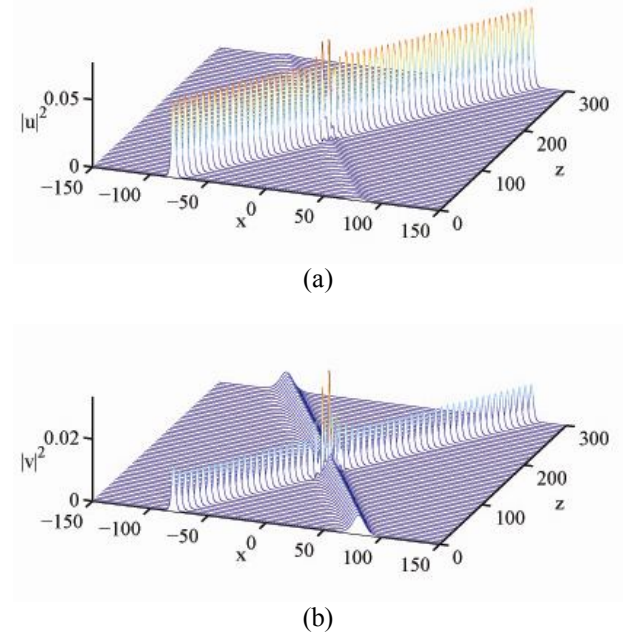


**Fig. 14.** (Color online) The collision between two stable moving solitons at  $\kappa - 1 = 0.2$  and  $Z_{\text{map}} = 0.5$ . The initial parameters of the left and right solitons are, respectively,  $c = 0.6$ ,  $\delta = \pi/10$  and  $c = -0.5$ ,  $\delta = \pi/30$ .

In all cases considered in the framework of the present model, collisions between stable solitons and breathers were elastic. As shown in Figs. 13 and 14, this is true for the collisions between identical solitons moving with opposite velocities,  $\pm c$ , and for soliton pairs with different amplitudes and/or velocities. Fig. 15

additionally displays a typical example of the elastic collision between stable breathers. The elasticity of the collisions attests to the fact that the solitons and breathers that were identified as stable ones are indeed very robust objects.

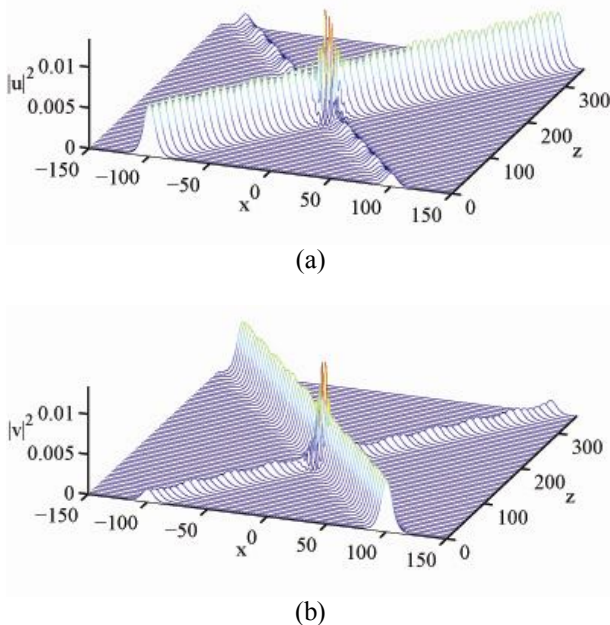


**Fig. 15.** (Color online) The collision between stable breathers moving with velocities  $c = \pm 0.6$ , the other parameters being  $\kappa - 1 = 0.2$ ,  $Z_{\text{map}} = 1.2$ , and  $\delta = \pi/30$ .

#### 4. CONCLUSION

In this work we have studied families of GSs (gap solitons) in the framework of the CME (coupled-mode equation) system in which the Bragg reflectivity was made a piecewise-constant function of the evolution variable. We have adopted the management map (3), with the reflectivity periodically switching off and on. The model may be realized in a straightforward way in a nonlinear planar waveguide, with the grating represented by an array of parallel dashed lines (grooves). In the temporal domain, a similar CME system was derived as a limit form of the model for BEC loaded into a rocking optical lattice. By dint of systematic simulations, which made use of the initial conditions corresponding to the exact GS solutions in the averaged version of the model, we have identified four different types of the dynamical behavior of the solitons (fully stable, weakly unstable, moderately unstable, and completely unstable). This was done for the quiescent and moving solitons (actually, untilted and tilted ones) alike. The weakly and moderately unstable solitons turn themselves into

persistent breathers (in the latter case, the breather features an erratic motion with a small velocity). Stability regions for the solitons and breathers have been identified. It was concluded that collisions between stable moving solitons and breathers are always elastic.

#### REFERENCES

- [1] R. Kashyap, *Fiber Bragg gratings* Academic Press: San Diego, 1999.
- [2] B. J. Eggleton, A. Ahuja, P. S. Westbrook, J. A. Rogers, P. Kuo, T. N. Nielsen, and B. Mikkelsen, "Integrated tunable fiber gratings for dispersion management in high-bit rate systems," *J. Lightwave Tech.* 18, 1418-1432, 2000.
- [3] H. G. Winful, J. H. Marburger, and E. Garmire, "Theory of bistability in nonlinear distributed feedback structures," *Appl. Phys. Lett.* 35, 379-381, 1979.
- [4] Yu. I. Voloshchenko, Yu. N. Ryzhov, and V. E. Sotin, "Stationary waves in nonlinear, periodically modulated media with large group retardation," *Zh. Tekh. Fiz.* 51, 902 (1981) *Sov. Phys. Tech. Phys.* 26, 541, 1981.
- [5] W. Chen and D. L. Mills, "Gap solitons and the nonlinear-optical response of superlattices," *Phys. Rev. Lett.* 58, 160-163, 1987.
- [6] C. M. de Sterke and J. E. Sipe, "Gap solitons", in *Progress in Optics*, E. Wolf, ed. (North-Holland, Amsterdam, 1994), Vol. XXXIII, Chap. III, pp. 203-260.
- [7] Y. S. Kivshar and G. P. Agrawal. *Optical Solitons* Academic Press: San Diego, 2003.
- [8] D. N. Christodoulides and R. I. Joseph, "Slow Bragg solitons in nonlinear periodic structure," *Phys. Rev. Lett.* 62, 1746-1749, 1989.
- [9] A. B. Aceves and S. Wabnitz, "Self-induced transparency solitons in nonlinear refractive periodic media," *Phys. Lett. A* 141, 37-42, 1989.
- [10] B. A. Malomed and R. S. Tasgal, "Vibration modes of a gap soliton in a nonlinear optical medium," *Phys. Rev. E* 49, 5787-5796, 1994.
- [11] I. V. Barashenkov, D. E. Pelinovsky, and E. V. Zemlyanaya, "Vibrations and Oscillatory Instabilities of Gap Solitons," *Phys. Rev. Lett.* 80, 5117-5120, 1998.
- [12] A. De Rossi, C. Conti, and S. Trillo, "Stability, multistability, and wobbling of optical gap solitons," *Phys. Rev. Lett.* 81, 85-88, 1998.
- [13] B. J. Eggleton, R. E. Slusher, C. M. de Sterke, P. A. Krug, and J. E. Sipe, "Bragg grating solitons," *Phys. Rev. Lett.* 76, 1627-1630, 1996.

- [14] B. J. Eggleton, C. M. De Sterke, and R. E. Slusher, "Bragg solitons in the nonlinear Schrödinger limit: experiment and theory," *J. Opt. Soc. Am. B* 16, 587-599, 1999.
- [15] J. T. Mok, C. M. de Sterke, I. C. M. Litte, and B. J. Eggleton, "Dispersionless slow light using gap solitons," *Nature Physics* 2, 775-780, 2006.
- [16] A. A. Sukhorukov and Yu. S. Kivshar, "Discrete gap solitons in modulated waveguide arrays," *Opt. Lett.* 27, 2112-2114, 2002.
- [17] P. G. Kevrekidis, B. A. Malomed, and Z. Musslimani, "Discrete gap solitons in a diffraction-managed waveguide array," *Eur. Phys. J. D* 23, 421-236, 2003.
- [18] D. Mandelik, H. S. Eisenberg, Y. Silberberg, R. Morandotti, and J. S. Aitchison, "Band-gap structure of waveguide arrays and excitation of Floquet-Bloch solitons," *Phys. Rev. Lett.* 90, 053902, 2003.
- [19] D. Mandelik, R. Morandotti, J. S. Aitchison, and Y. Silberberg, "Gap Solitons in Waveguide Arrays," *Phys. Rev. Lett.* 92, 093904, 2004.
- [20] F. Chen, M. Stepić, C. E. Rüter, D. Runde, D. Kip, V. Shandarov, O. Manela, and M. Segev, "Discrete diffraction and spatial gap solitons in photovoltaic LiNbO<sub>3</sub> waveguide arrays," *Opt. Exp.* 13, 4314-4324, 2005.
- [21] J. W. Fleischer, T. Carmon, M. Segev, N. K. Efremidis, and D. N. Christodoulides, "Observation of discrete solitons in optically induced real time waveguide arrays," *Phys. Rev. Lett.* 90, 023902, 2003.
- [22] D. Neshev, A. A. Sukhorukov, B. Hanna, W. Krülikowski, and Yu. S. Kivshar, "Controlled generation and steering of spatial gap solitons," *Phys. Rev. Lett.* 93, 083905, 2004.
- [23] W. Fleischer, M. Segev, N. K. Efremidis, and D. N. Christodoulides, "Observation of two-dimensional discrete solitons in optically induced nonlinear photonic lattices," *Nature* 422, 147-150, 2003.
- [24] J. Feng, "Alternative scheme for studying gap solitons in an infinite periodic Kerr medium," *Opt. Lett.* 18, 1302-1304, 1993.
- [25] R. F. Nabiev, P. Yeh, and D. Botez, "Spatial gap solitons in periodic nonlinear structures," *Opt. Lett.* 18, 1612-1614, 1993.
- [26] W. C. K. Mak, B. A. Malomed, and P. L. Chu, "Three-wave gap solitons in waveguides with quadratic nonlinearity," *Phys. Rev. E* 58, 6708-6722, 1998.
- [27] F. Biancalana, A. Amann, and E. P. O'Reilly, "Gap solitons in spatiotemporal photonic crystals," *Phys. Rev. A* 77, 011801(R), 2008.
- [28] P. St. J. Russell, "Optical superlattices for modulation and deflection of light," *J. Appl. Phys.* 59, 3344-3355, 1986.
- [29] N. G. R. Broderick and C. M. de Sterke, "Theory of grating superstructures," *Phys. Rev. E* 55, 3634-3646, 1977.
- [30] J. B. Khurgin, "Light slowing down in Moiré fiber gratings and its implications for nonlinear optics," *Phys. Rev. A* 62, 013821, 2000.
- [31] R. Shimada, T. Koda, T. Ueta, and K. Ohtaka, "Strong localization of Bloch photons in dual-periodic dielectric multilayer structures," *J. Appl. Phys.* 90, 3905, 2001.
- [32] D. Janner, G. Galzerano, G. Della Valle, P. Laporta, S. Longhi, and M. Belmonte, "Slow light in periodic superstructure Bragg gratings," *Phys. Rev. E* 72, 056605, 2005.
- [33] K. Levy, B. A. Malomed, "Stability and collisions of traveling solitons in Bragg-grating superstructures," *J. Opt. Soc. Am. B* 25, 302, 2008.
- [34] K. Yagasaki, I. M. Merhasin, B. A. Malomed, T. Wagenknecht, and A. R. Champneys, "Gap solitons in Bragg gratings with a harmonic superlattice," *Europhys. Lett.* 74, 1006-1012, 2006.
- [35] T. Mayteevarunyoo and B. A. Malomed, "Gap solitons in grating superstructures," *Opt. Exp.* 16, 7767-7777, 2008.
- [36] P. J. Y. Louis, E. A. Ostrovskaya, and Y. S. Kivshar, "Dispersion control for matter waves and gap solitons in optical superlattices," *Phys. Rev. A* 71, 032612, 2005.
- [37] J. Atai and B. A. Malomed, "Spatial solitons in a medium composed of self-focusing and self-defocusing layers," *Phys. Lett. A* 298, 140-148, 2002.
- [38] B. A. Malomed, *Soliton Management in Periodic Systems* Springer: New York, 2006.
- [39] H. Lignier, C. Sias, D. Ciampini, Y. Singh, A. Zenesini, O. Morsch, and E. Arimondo, "Dynamical control of matter-wave tunneling in periodic potentials," *Phys. Rev. Lett.* 99, 220403, 2007.
- [40] A. Eckardt, M. Holthaus, H. Lignier, A. Zenesini, D. Ciampini, O. Morsch, and E. Arimondo, "Exploring dynamic localization with a Bose-Einstein condensate," *Phys. Rev. A* 79, 013611, 2009.
- [41] F. Dreisow, A. Szameit, M. Heinrich, T. Pertsch, S. Nolte, and A. Tünnermann, and S. Longhi, "Decay control via discrete-to-continuum coupling modulation in an optical waveguide system," *Phys. Rev. Lett.* 101, 143602, 2008.

- [42] T. Mayteevarunyoo and B. A. Malomed, "Gap solitons in rocking optical lattices and waveguides with undulating gratings," *Phys. Rev. A* 80, 013827, 2009.
- [43] W. C. K. Mak, B. A. Malomed, and P. L. Chu, "Slowdown and splitting of gap solitons in apodized Bragg gratings," *J. Mod. Opt.* (51) 2141-2158, 2004.
- [44] W. C. K. Mak, B. A. Malomed, and P. L. Chu, "Formation of a standing-light pulse through collision of gap solitons," *Phys. Rev. E* 68, 026609, 2003.
- [45] D. R. Neill and J. Atai, "Collision dynamics of gap solitons in Kerr media," *Phys. Lett. A* 353, 416-421, 2006.
- [46] D. R. Neill, J. Atai, and B. A. Malomed, "Dynamics and collisions of moving solitons in Bragg gratings with dispersive reflectivity," *J. Opt. A: Pure Appl. Opt.* 10, 085105, 2008.



**Boris Malomed** was born in Minsk (ex-USSR) in 1955. He had received his M.S. in physics from the Byelorussian State University in 1977, Ph.D. in theoretical physics from the Moscow Physico-Technical Institute in 1981, and the D.Sc. degree in theoretical physics (second doctorate/habilitation)

from the Institute for Theoretical Physics of the Ukrainian Academy of Sciences (Kiev) in 1989. Till 1991, he was a senior researcher at the Institute for Oceanology of the Russian Academy of Sciences (Moscow). He joined the Tel Aviv University in 1991, first the Department of Applied Mathematics, and then the Faculty of Engineering (Department of Physical Electronics), where he became a full professor in 1999. His research interests are in the fields of solitons and nonlinear waves in various physical media, especially in optics and Bose-Einstein condensates, and also include nonlinear pattern formation in dissipative media (the theory of Ginzburg-Landau equations), optical telecommunications, Josephson junctions, superconductivity, and some other topics. Since May 2009, he serves as a Divisional Associate Editor of *Physical Review Letters*. He was awarded with the title of the "Outstanding Referee of the American Physical Society". He has about 700 scientific publications, including a book, "Soliton Management in Periodic Systems" (Springer-US, 2006). His current personal Hirsch-factor is 49.